Special Issue: Research Article

polymers advanced technologies

Received: 31 December 2007, Revised: 17 June 2008, Accepted: 23 June 2008, Published online in Wiley InterScience: 8 October 2008

(www.interscience.wiley.com) DOI: 10.1002/pat.1257

Thermal annealing behavior of silica-coated coaxial nanowires†

Hyoun Woo Kim[a]*, Jong Woo Lee[a], Changmu Lee[a] and Mesfin A. Kebede[a]

The effects of thermal annealing on structural and optical properties of MgO-core–silica (SiO_x)-shell nanowires have been investigated. The annealed nanostructures consisted of a crystalline MgO core surrounded by an amorphous SiO_x shell layer, whereas the shell surface had become rough and an Mg_2SiO_4 phase appeared by annealing at a sufficiently high temperature of 800°C. Photoluminescence (PL) measurements of annealed MgO-core/SiO_x-shell nanowires indicated that the overall intensities increased on increasing the annealing temperature, with the overall shapes of the emission spectra being independent of the annealing temperature from 600 to 1000°C. This study provides an insight into the annealing studies involving various coaxial nanowires. Copyright © 2008 John Wiley & Sons, Ltd.

Keywords: nanotechnology; silica; annealing

INTRODUCTION

In recent years, coaxial one-dimensional (1D) structures have begun to attract interest because their functions could be further enhanced by fabricating core and sheath from different materials in the radial direction.[1–3] In particular, coating of nanostructures with silica (SiO_x) in the form of amorphous inorganic polymer has numerous advantages,[4–6] including insulating characteristics, protection from contamination, and chemical stability for preventing their aggregation in liquid. Also, SiO_x surface can be easily functionalized with various coupling reagents, which allows robust attachment of a variety of specific ligands.[7,8] Furthermore, the SiO_x coating layer does not degrade the intrinsic optical properties of core materials owing to its optical transparency for the visible absorption and emission regions of the spectra.[7,9]

In the present work, the MgO nanowires have been coated by a sputtering technique to fabricate MgO/SiO_x core–shell nanowires. MgO is an important material for such applications as catalysis, superconductor products, and optoelectronics.[10–12] Since both MgO and SiO_x are crucial materials for industrial applications and are of scientific interest, this efficient fabrication approach will pave the way for potential applications of core–shell nanowires. Furthermore, MgO nanowires are easy to prepare and are suitable for use in sacrificial templates, which can be easily removed by dipping them in a dilute $(NH_3)_2SO_4$ solution to obtain hollow SiO_x nanotubes.

Although a variety of materials, such as Ag,[13] InS,[5] and CdTe,[6] have been utilized as cores in core–shell nanowires comprising an SiO_x shell layer, there has not been any report so far on modification of the SiO_x shell by thermal annealing. Herein, the effects of thermal annealing on the morphology, structure, and optical properties of MgO/SiO_x core–shell nanowires have been investigated. Since these structures will be used as building blocks in future ultra-large-scale-integration fabrication, in which inter-wire spacing, insulating properties, and the protectability could be easily achieved by coating the SiO_x shell layers,[13] it is crucial to investigate the thermal annealing behavior, which will subsequently undergo high-temperature fabrication processes.

EXPERIMENTAL

MgO core nanowires were prepared by evaporating pure MgB_2 powders in a high-temperature quartz tube furnace. The temperature in the furnace was set to 900°C for 1 hr, in a flow of Ar/O_2 gas mixture. Detailed experimental procedures were previously reported.[14] Subsequently, coating experiments were carried out on the as-prepared MgO nanowires using a turbo sputter coater (Emitech K575X, Emitech Ltd., Ashford, Kent, UK). A piece of polished *p*-type (100) Si wafer (1–30 Ω cm) was used as a sputtering target.[15] The sputtering was performed at room temperature with the flow of Ar gas at a pressure of 8×10^{-4} Pa. The DC sputtering current and the sputter time were about 120 mA and 1 min, respectively. Following this, the samples were subjected to thermal annealing in a quartz tube furnace in N_2 ambient for 1 hr (flow rate: 500 standard cm^3/min). The annealing temperature was set to 600, 800, and 1000°C, respectively. Although a nearly pure Ar atmosphere was used during the sputtering process, it is surmised that oxygen in SiO_x layers comes from Ar gas, Si wafer surface, and from the inside of the chamber.

* *Correspondence to: H. W. Kim, Division of Materials Science and Engineering, Inha University, Incheon 402751, Republic of Korea.*
E-mail: hwkim@inha.ac.kr

a *H. W. Kim, J. W. Lee, C. Lee, M. A. Kebede*
Division of Materials Science and Engineering, Inha University, Incheon 402751, Republic of Korea

Contract/grant sponsor: Inha University Research Grant.
Contract/grant sponsor: Korea Research Foundation Grant; contract/grant number: Korean Government (MOEHRD) KRF-2007-521-D00216.

† *The main calculations were performed by the supercomputing resources of the Korea Institute of Science and Technology Information (KISTI).*

The products were characterized by a glancing angle (0.5°) X-ray diffraction (XRD) (Philips X'pert MRD diffractometer with Cu$K\alpha_1$ radiation) with the contribution from the substrate minimized, scanning electron microscopy (SEM) (Hitachi, S-4200), and transmission electron microscopy (TEM) (Philips, CM-200) being equipped with an energy-dispersive X-ray (EDX) spectrometer. Photoluminescence (PL) measurement was conducted at room temperature on an SPEC-1403 PL spectrometer with a 325 nm line from a He-Cd laser (Kimon, 1K, Japan).

RESULTS AND DISCUSSION

Figure 1(a)–1(c) displays typical top-view SEM images of as-deposited, 600°C-annealed, and 800°C-annealed MgO/SiO_x core–shell nanowires, respectively. The images indicate that products consist of 1D structures, regardless of the annealing temperature. Figure 1(c) shows that the surface of nanowires is bound to be rough as a result of the thermal annealing with a sufficiently high temperature of 800°C. Figure 2(a)–2(d) shows

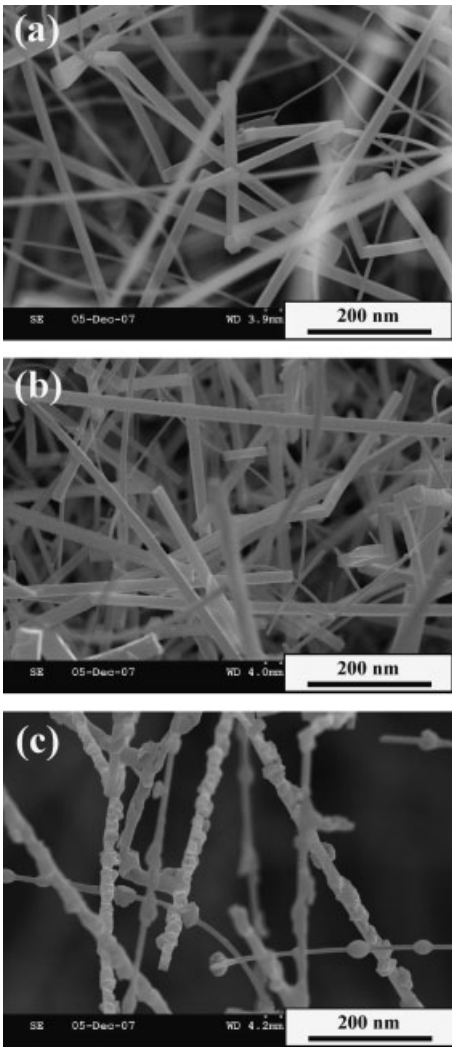

Figure 1. Top-view SEM images of (a) as-synthesized, (b) 600°C-annealed, and (c) 800°C-annealed MgO/SiO_x core–shell nanowires.

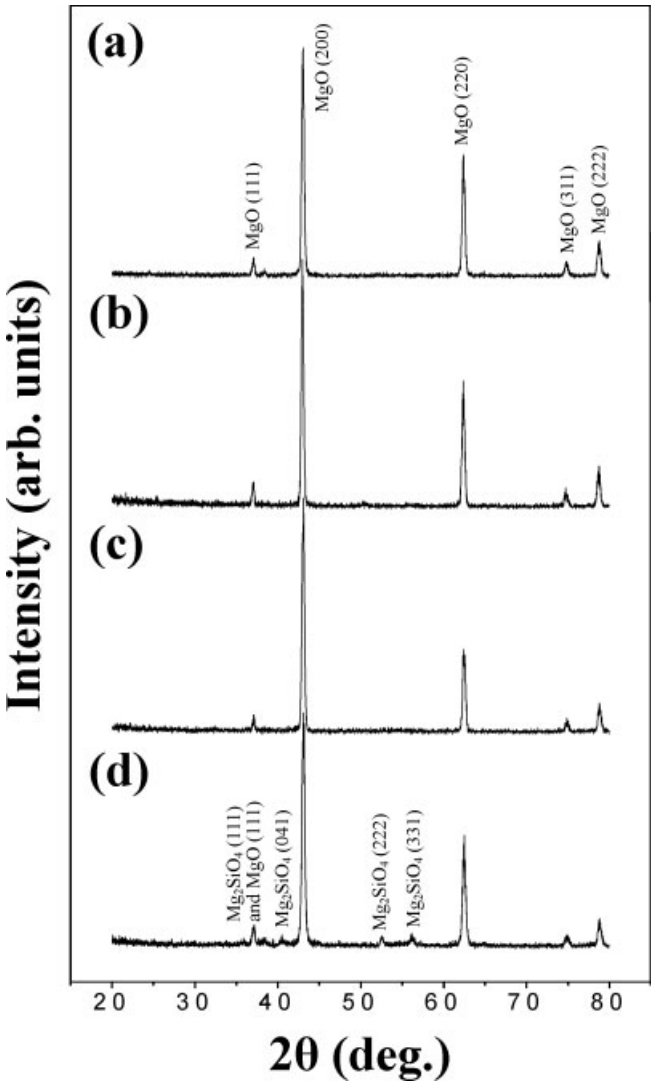

Figure 2. XRD patterns of (a) core MgO nanowires, (b) as-deposited core–shell nanowires, (c) 600°C-annealed core–shell nanowires, and (d) 800°C-annealed core–shell nanowires.

XRD patterns of core MgO nanowires, as-deposited core–shell nanowires, 600°C-annealed, and 800°C-annealed core–shell nanowires, respectively. Figure 2(a) indicates that all recognizable diffraction peaks of core nanowires can be indexed to cubic MgO with a lattice constant comparable to the value of JCPDS 04-0829. The SiO_x-coating does not significantly change the XRD spectrum (Fig. 2(b)), suggesting that the coated shell layer is amorphous in nature. On the other hand, although annealed samples mainly comprise an MgO phase regardless of annealing temperature (Fig. 2(c) and 2(d)), it is worthwhile to note that an Mg_2SiO_4 phase is found from the XRD spectra of annealed samples at a relatively high annealing temperature of 800°C (Fig. 2(d)). For samples annealed at 800–1000°C, there existed weak diffraction peaks corresponding to the orthorhombic Mg_2SiO_4 structure with lattice parameters of $a = 5.982$ Å, $b = 10.198$ Å, and $c = 4.755$ Å (JCPDS: 34-0189). Since a 600°C-annealed sample does not comprise the Mg_2SiO_4 phase (Fig. 2(c)), it is suggested that Mg_2SiO_4 phase has been generated due to the reaction of SiO_x and MgO at a sufficiently high temperature.

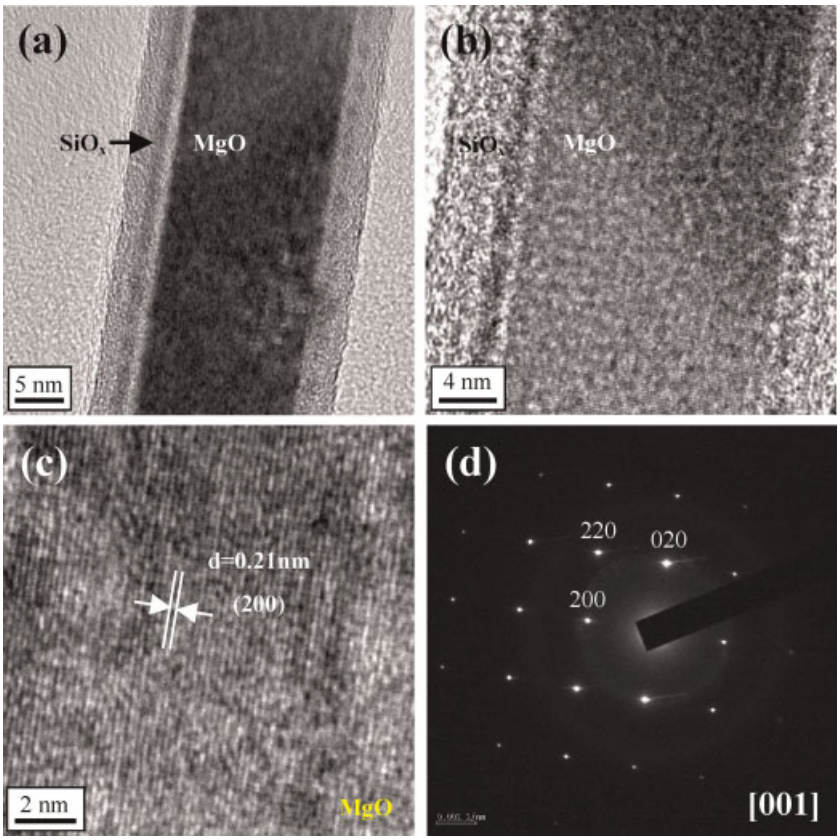

Figure 3. (a) TEM image of a MgO/SiO$_x$ core–shell nanowire prior to thermal annealing. (b) TEM image showing an enlargement of core and shell regions. (c) Lattice-resolved TEM image enlarging a core region in (b). (d) Corresponding SAED pattern. This figure is available in color online at www.interscience.wiley.com/journal/pat

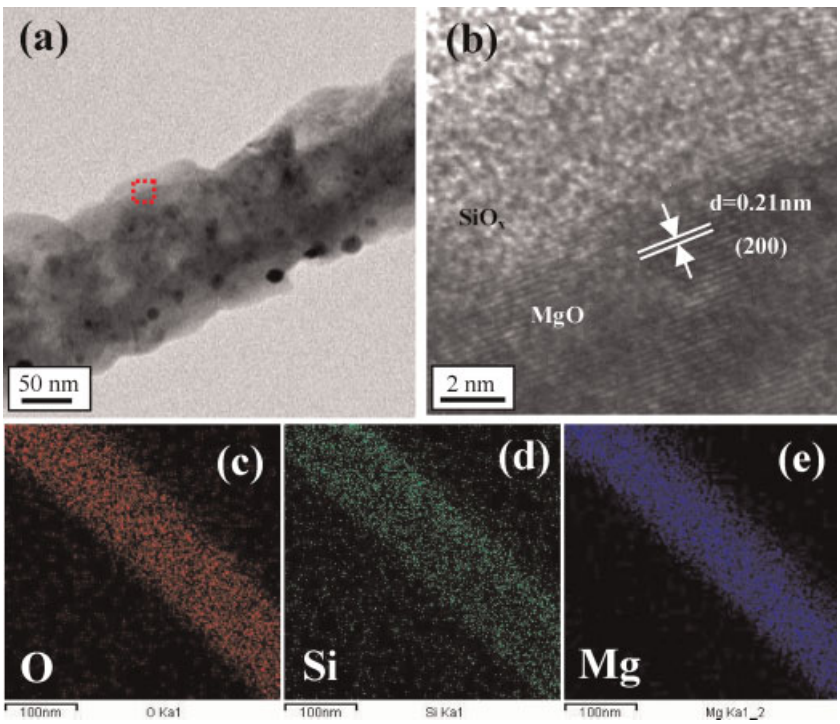

Figure 4. (a) TEM image of a MgO/SiO$_x$ core–shell nanowire after thermal annealing at 800°C. (b) Lattice-resolved TEM image enlarging a region enclosed by square box in (a). TEM elemental maps of (c) O, (d) Si, and (e) Mg concentrations from an annealed MgO/SiO$_x$ core–shell nanowire. This figure is available in color online at www.interscience.wiley.com/journal/pat

Figure 3(a) exhibits a TEM image of a MgO/SiO_x core–shell nanowire prior to thermal annealing, clearly indicating that there are two segments in the structure: a rod-like core and thin coating layers (on both sides). The shell layer is relatively smooth and continuous along the nanowire. An enlarged TEM image as shown in Fig. 3(b) reveals that the shell and the core are amorphous and crystalline, respectively. Lattice-resolved TEM image (Fig. 3(c)) reveals that an interplanar spacing of the core region is approximately 0.21 nm, corresponding to the (2 0 0) plane of cubic MgO. Figure 3(d) shows the associated selected area electron diffraction (SAED) pattern, showing a set of single-crystal electron diffraction spots corresponding to the MgO core, with the amorphous nature of shell layer not contributing the diffraction ring or spot to the SAED pattern.

Figure 4(a) shows a low-magnification TEM image of an MgO/SiO_x core–shell nanowire after thermal annealing at 800°C. The nanowire shows a rough surface, which is in good agreement with the SEM observation. Figure 4(b) is a lattice-resolved TEM image showing an enlargement of the area enclosed by the dotted square in Fig. 4(a). While the shell is not crystalline, the interplanar spacing in the core region corresponds to the (2 0 0) plane of cubic MgO. Figure 4(c)–4(e) corresponds to TEM–EDX elemental mapping of the O, Si, and Mg concentrations, respectively, in an annealed core–shell nanowire. Since the core nanowire corresponds to pure MgO, the shell layer is supposed to comprise Si elements, from the existence of bright points in the Si elemental mapping (Fig. 4(d)). As the diameter of the O elemental map (Fig. 4(c)) is apparently larger than that of the Mg elemental map (Fig. 4(e)), it is revealed that O is also present at the shell part of the nanowire. Accordingly, TEM and EDX analyses are in good agreement with what can be expected for the SiO_x-coated MgO nanowires. Since high-temperature annealing being carried out under the same conditions on core MgO nanowires generated a smooth surface (not shown here), the surface-roughening of the core–shell nanowires (as shown in Fig. 1(c) and 4(a)) is presumably due to changes in the shape of the SiO_x shell layer. Although thermal annealing may induce the structural changes in SiO_x via a variety of processes such as rearrangement of atoms, density change, and phase transition or transformation,[16,17] further study is underway to explore a detailed mechanism. It is expected that a rough surface may have potential applications due to its high surface area and catalytic activity for important chemical reactions.

Figure 5(a) and 5(b) shows the room-temperature PL emission spectra of annealed MgO/SiO_x core–shell nanowires with an annealing temperature of 600 and 1000°C, respectively, indicating that the overall PL intensity has been increased by increasing the annealing temperature. Figure 5(c) and 5(d) shows the results of a Gaussian fitting analysis of the normalized PL spectra of 600°C-annealed and 1000°C-annealed MgO/SiO_x core–shell nanowires, respectively. Not only overall shape but also peak positions have not significantly been changed by varying the annealing temperature. The best fit of the emission from both Fig. 5(c) and 5(d) has been obtained with five Gaussian functions, which are centered at 2.0, 2.3, 2.7, 2.8, and 3.0 eV, respectively. It is suggested that two peaks at 2.7 eV in the blue region and 2.3 eV in the green region originate from MgO core nanowires. Blue[18,19] and green[20] emissions have been previously observed in the PL spectra from MgO nanostructures. Both blue and green light emissions may originate from defects in MgO, such as oxygen vacancy,[21] Mg vacancies, and interstitials.

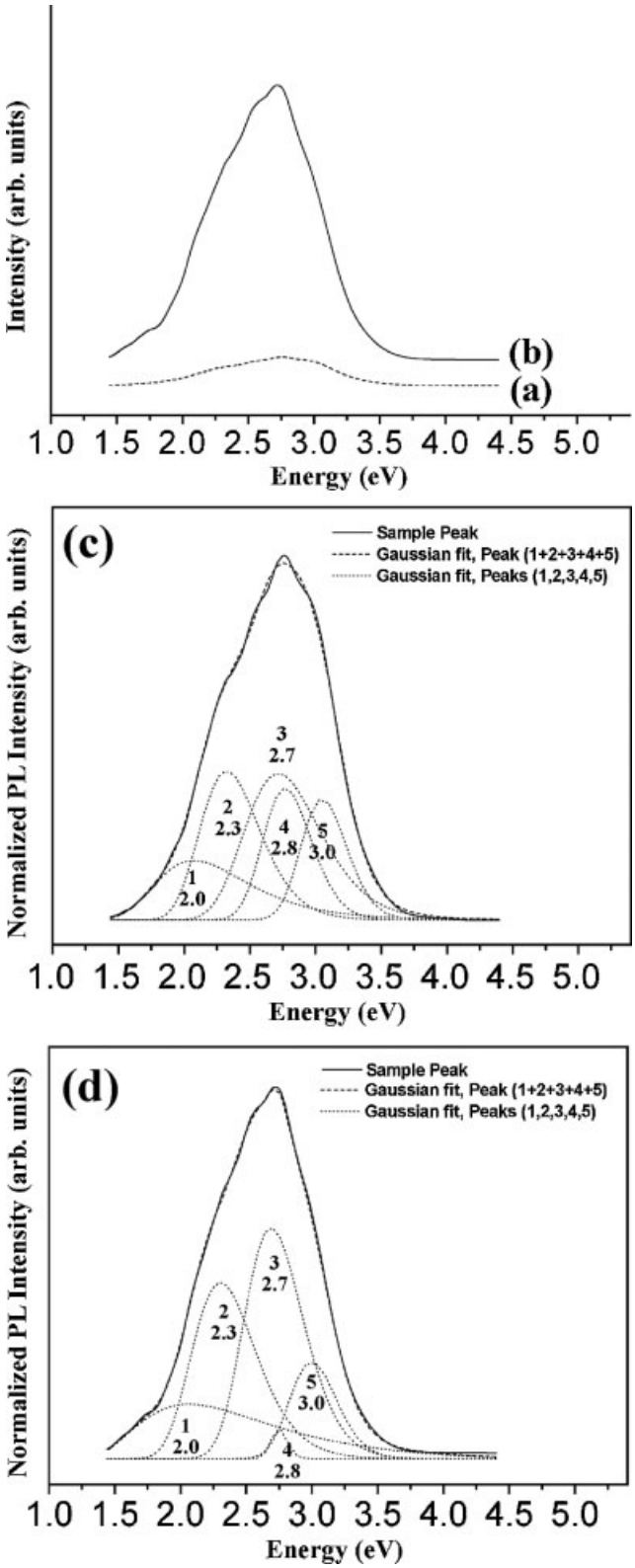

Figure 5. Room-temperature PL emission spectra of annealed MgO/SiO_x core–shell nanowires with an annealing temperature of (a) 600°C and (b) 1000°C. Gaussian fitting analyses of (c) 600°C- and (d) 1000°C-annealed samples, indicating that both emission bands are superimposition of five emission peaks.

In addition, there exists three additional peaks: first, being similar to the emission band peaked at about 2.8 eV, the blue emission has previously been observed from amorphous SiO_x nanowires, which is attributed to the neutral oxygen vacancy (=Si–Si=).[22–25] Second, we surmise that the violet emission at approximately 3.0 eV originates from the SiO_x sheath layer, as similar violet emission bands have been observed from SiO_x nanowires.[22,23,25] This violet emission is ascribed to an intrinsic diamagnetic defect center, such as the twofold coordinated silicon lone pair centers (O–Si–O), which are associated with the high oxygen deficiency in SiO_x.[23,25] Third, there is a weak and broad emission band peaked at around 2.0 eV in the yellow region. Similar emissions in the range of 1.9–2.1 eV have been observed from silica in the form of bulk,[26,27] films,[28,29] and nanowires.[30] It is suggested that the yellow emission is attributed to defects such as non-bridging oxygen hole centers.[27,31] Further study is necessary for revealing the exact origin of associated defects.

Since the shape and peak positions of PL spectra have not been noticeably changed by varying the annealing temperature from 600 to 1000°C, it is expected that there is almost no or negligible contribution from the Mg_2SiO_4 phase, which has been generated due to thermal annealing at a sufficiently high temperature. Also, the overall PL intensity was considerably enhanced by increasing the annealing temperature (Fig. 5(a) and 5(b)), suggesting that a higher temperature annealing process may facilitate the generation of various defects.

CONCLUSION

It has been revealed that the application of a thermal annealing process has induced changes in the characteristics of SiO_x-coated MgO nanowires. XRD spectra show that the products mainly comprise a cubic MgO phase regardless of the annealing temperature, whereas a Mg_2SiO_4 phase has been found from the XRD spectra of annealed samples at a relatively high annealing temperature of 800°C. The shell surface becomes rough due to the thermal annealing at a relatively high annealing temperature. With the possible emission mechanisms being discussed, it is suggested that the PL emission of annealed MgO-core/SiO_x-sheath nanowires comprises emissions from the SiO_x sheath as well as those from the MgO-core nanowires. Thermal annealing at higher temperature enhances the overall PL intensity, presumably being attributed to an increase in the amount of defects.

REFERENCES

[1] Y. Wu, J. Xiang, C. Yang, W. Lu, C. M. Lieber, *Nature* **2004**, *43*, 61–65.
[2] L. J. Lauhon, M. S. Gudiksen, D. Wang, C. M. Lieber, *Nature* **2002**, *42*, 57–61.
[3] H. J. Choi, J. C. Johnson, R. He, S. K. Lee, F. Kim, P. Pauzauskie, J. Golberger, R. J. Saykally, P. Yang, *J. Phys. Chem. B* **2003**, *10*, 8721–8725.
[4] Y. Zhang, K. Suenage, C. Colliex, S. Iijima, *Science* **1998**, *28*, 973–975.
[5] Y. B. Li, Y. Bando, D. Golberg, Y. Uemura, *Appl. Phys. Lett.* **2003**, *8*, 3999–4001.
[6] Y. Wang, Z. Tang, X. Liang, L. M. Liz-Marzan, N. A. Kotov, *Nano Lett.* **2004**, *281*, 225–231.
[7] A. Schroedter, H. Weller, R. Eritja, W. E. Ford, J. M. Wessels, *Nano Lett.* **2002**, *83*, 1363–1367.
[8] M. Bruchez, Jr., M. Moronne, P. Gin, S. Weiss, A. P. Alivisatos, *Science* **1998**, *28*, 2013–2016.
[9] A. Pan, S. Wang, R. Liu, C. Li, B. Zou, *Small* **2005**, *1*, 1058–1062.
[10] S. H. C. Liang, I. D. Gay, *J. Catal.* **1986**, *10*, 293–300.
[11] P. D. Yang, C. M. Lieber, *Science* **1996**, *27*, 1836–1840.
[12] G. P. Summers, T. M. Wilson, B. T. Jeffries, H. T. Tohver, Y. Chen, M. M. Abraham, *Phys. Rev. B* **1983**, *2*, 1283–1291.
[13] Y. Yin, Y. Lu, Y. Sun, Y. Xia, *Nano Lett.* **2002**, *2*, 427–430.
[14] H. W. Kim, S. H. Shim, *Chem. Phys. Lett.* **2006**, *42*, 165–169.
[15] H. W. Kim, S. H. Shim, J. W. Lee, *Carbon* **2007**, *4*, 2695–2698.
[16] A. Takada, P. Ricket, C. R. A. Catlow, G. D. Proce, *J. Non-Cryst. Solids* **2008**, *35*, 181–187.
[17] S. Sen, *J. Phys. Chem. B* **2007**, *11*, 9431–9433.
[18] F. L. Deepak, P. Saldanha, S. R. C. Vivekchand, A. Govindaraj, *Chem. Phys. Lett.* **2006**, *41*, 535–539.
[19] K. P. Kalyanikutty, F. L. Deepak, C. Edem, A. Govindaraj, C. N. R. Rao, *Mater. Res. Bull.* **2005**, *4*, 831–839.
[20] J. Zhang, L. Zhang, *Chem. Phys. Lett.* **2002**, *36*, 293–297.
[21] G. H. Rosenblatt, M. W. Rowe, G. P. Williams, Jr., R. T. Williams, Y. Chen, *Phys. Rev. B* **1989**, *3*, 10309–10318.
[22] X. C. Wu, W. H. Song, K. Y. Wang, T. Hu, B. Zhao, Y. P. Sun, J. J. Du, *Chem. Phys. Lett.* **2001**, *33*, 53–56.
[23] K. H. Lee, S. W. Lee, R. R. Vanfleet, W. Sigmund, *Chem. Phys. Lett.* **2003**, *37*, 498–503.
[24] H. Nishikawa, T. Shiroyama, R. Nakamura, Y. Ohki, K. Nagasawa, Y. Hama, *Phys. Rev. B* **1992**, *4*, 586–591.
[25] D. P. Yu, Q. L. Hang, Y. Ding, H. Z. Zhang, Z. G. Bai, J. J. Wang, Y. H. Zou, W. Qian, G. C. Xiong, S. Q. Feng, *Appl. Phys. Lett.* **1998**, *7*, 3076–3078.
[26] A. Paleari, N. Chiodini, D. Martino, F. Meinardi, P. Fumagalli, *Phys. Rev. B* **2003**, *68*, 184107-1–4.
[27] S. Juodkazis, M. Watanabe, H. B. Sun, S. Matsuo, J. Nishii, H. Misawa, *Appl. Surf. Sci.* **2000**, *154–15*, 696–700.
[28] H. Rinnert, M. Vergnat, G. Marchal, A. Burneau, *J. Lumin.* **1999**, *8*, 445–448.
[29] O. Jambois, M. Molinari, H. Rinnert, M. Vergnat, *Opt. Mater.* **2005**, *2*, 1074–1078.
[30] J. Niu, J. Sha, N. Zhang, Y. Ji, X. Ma, D. Yang, *Physica E.* **2004**, *2*, 1–4.
[31] L. Skuja, *J. Non-Cryst. Solids* **1998**, *23*, 16–48.